Photoacoustic imaging of blood vessel equivalent phantoms

Beard PC[1]

Department of Medical Physics and Bioengineering, University College London, Shropshire House, 11-20 Capper Street, London WC1E 6JA, UK

ABSTRACT

Various phantoms have been used to assess the ability of transmission mode photoacoustic imaging to visualise blood vessels. A Q switched Nd:YAG laser operating at 1.06μm was used as the pulsed excitation source. The surface distribution of the photoacoustic signals was mapped by mechanically scanning a photodiode across the reflected output beam of a Fabry Perot polymer film ultrasound sensor. The depth profile of a 1.3mm thick polymer sheet (μ_a=0.8mm^{-1}) immersed to a depth of 2cm in an Intralipid scattering solution (μ_s'=1mm^{-1}, μ_a=0.03mm^{-1}) was imaged using a 1D detector scan and a simple line-of-sight approach to image reconstruction. An arrangement comprising three 3 lines of PMMA tubing of internal diameter 62.5μm, arranged at different heights and filled with human blood, was immersed to depths of up to 7mm in the Intralipid solution. Using a radial backprojection algorithm, 2D and 3D images were reconstructed from 1D and 2D detector scans respectively. The "vessels" could be observed as high contrast features on the images. Lateral resolution, limited by the detector aperture was 0.33mm and the axial resolution was 0.15mm.

Keywords: Photoacoustic, thermoacoustic, imaging, microvasculature, ultrasound array, biomedical, Fabry Perot sensor.

1. INTRODUCTION

Photoacoustic or thermoacoustic imaging is a soft tissue imaging modality in which sub-microsecond pulses of optical or microwave electromagnetic radiation are used to excite subsurface acoustic waves on to which the spatial and functional properties of the tissue are encoded. The signal generation process is one in which the absorption of the incident pulsed radiation leads to impulsive heating of the irradiated tissue volume followed by rapid thermoelastic expansion and the subsequent generation of broadband ultrasonic thermoelastic waves. These propagate to the surface where they are detected by an array of ultrasound transducers. The detected signals can then be spatially resolved and back-projected in 3 dimensions to reconstruct a volumetric image of the internally absorbed electromagnetic energy distribution from which a 3D representation of the internal tissue structure can be extracted. The penetration depths that can be achieved depends upon the attenuation of the excitation radiation in the tissue and the signal losses due to frequency dependent attenuation of ultrasound in tissue with the latter also determining spatial resolution. Depths of several cm with mm spatial resolution using both microwave[1] and NIR (near-infrared) laser excitation[2] have been reported for applications such as breast imaging for the detection of cancerous lesions. Higher spatial resolution (<100μm) has been demonstrated with sub-cm penetration depths for applications such as imaging skin and superficial blood vessels[3,4].

The potential for high contrast is possibly the most widely proffered advantage of the technique. This is particularly so when optical excitation is used as it enables the large variation in the optical absorption and scattering properties of different tissue constituents to be exploited. Sources of naturally occurring absorption contrast include chromophores such as haemoglobin (and its various oxygenated states), melanin, beta-carotene, lipids whilst scattering based contrast arises from the presence of fibrous tissue, collagen, increased cellularity, and calcification. Of all of these, haemoglobin is perhaps the most significant. It offers strong optical contrast at visible and NIR optical wavelengths making the technique particularly well suited to imaging the microvasculature (arterioles, venules and capillaries) - by contrast, conventional ultrasound imaging is

[1] Correspondence to P. Beard, Dept of Medical Physics, UCL, Shropshire House, 11-20 Capper Street, London WC1E 6JA, UK, email: pbeard@medphys.ucl.ac.uk, http://www.medphys.ucl.ac.uk/research/mle/research.htm

Proc. SPIE 4618, pp54-62, 2002
SPIE BIOS 2002, 20-21 January 2002, San Jose

limited by the relatively poor echogenicity of blood vessels. The spectroscopic nature of the technique also offers the prospect of exploiting the well established relationship between optical absorption and blood oxygenation to map the distribution of oxygen saturation[4] over microvessels. This dual spatial-spectroscopic ability offers a potentially powerful tool for physiological and clinical studies of, for example, abnormal tissue morphologies such as cancerous lesions that are characterised by changes in surrounding vasculature and local oxygenation status.

We have explored the potential for imaging blood vessels by obtaining photoacoustic images in transmission mode of various targets designed to mimic the optical and geometrical properties of blood vessels and their surrounding tissues. A key feature is a Fabry Perot polymer film detection system[5,6,7,8], described in section 2, that was used to map the photoacoustic signals arriving at the surface. In sections 3.1 and 3.2.1, images obtained using planar and cylindrical absorbers immersed in scattering media were used to assess penetration depth and spatial resolution. In section 3.2.2, 2D and 3D images of a network of thin (62.5μm) tubing containing human blood and immersed in scattering media are described.

2. PHOTOACOUSTIC IMAGING SYSTEM

Figure 1 shows a schematic of the experimental set-up used to obtain photoacoustic images in transmission mode: ie the incident excitation laser pulses are delivered to one side of the target and the photoacoustic signals detected on the other. The sensor head comprises a 75μm thick polyethylene terepthalate (PET) Fabry Perot polymer film sensing interferometer bonded to a 4mm thick impedance matched PMMA backing stub. An incident photoacoustic signal modulates the optical thickness and hence the reflectivity of the polymer film. The sensor is illuminated with a large area cw laser beam (12mm diameter) and a 25MHz pin photodiode is mechanically scanned under PC control over the reflected interferometer output beam. At each point of the scan, following the phase bias control procedure to optimise the sensitivity of the interferometer described below, the reflected intensity modulation due to the photacoustic signal is captured using a 500MHz digitising oscilloscope. In this way the temporal and lateral distribution of the incident acoustic field can be mapped and subsequently backprojected to reconstruct an image of the target. The detection sensitivity of the sensor was ~5kPa (over a 25MHz measurement bandwidth) and the frequency response 15MHz - a performance comparable to piezoelectric PVDF transducers[8,9]. Key advantages, in common with other optical methods[10,11], are the potential to achieve substantially smaller element sizes (in principle down to the optical diffraction limit of a few μm) and interelement spacings than are possible with piezoelectric arrays and implement a reflection-mode sensing configuration[17].

A difficulty with Fabry Perot sensing interferometers is the large variation in sensitivity across the sensor head[6] arising from changes in the interferometer phase bias due to changes in optical thickness. We have developed a means of overcoming this using an active angle-tuned phase bias control system. The system operates by adjusting the angle θ_o of the incident beam and therefore the optical path length of the interferometer enabling the phase bias to be controlled. This is achieved using a 1-1 beam expander arrangement comprising lenses L1 and L2 with a galvanometer mirror under PC control situated in the back focal plane of L1. The sensor is positioned in the front focal plane of L2 and the reflected output beam equivalently reversed through system by directing it through L3 and imaging it on to the mechanically scanned photodiode situated in focal plane of L3. All three lenses have the same focal length of 59mm. Changing the angle θ_i of the input beam using the galvanometer mirror produces a corresponding change in the angle θ_o of the light incident on the sensor without translating it across the surface. The light reflected from the sensor is imaged on to the photodiode, also without translation, as θ_i is varied. By ensuring that there is no lateral translation of the beam either at the acoustic (P1) or optical (P2) detection planes, the lateral spatial fidelity of the incident acoustic field is preserved. Using this system, the reflected interference fringes, the spatial derivatives of which can be thought of as contours of uniform sensitivity, can be scanned across the illuminated area of the sensor enabling each point to be interrogated with optimum sensitivity.

In practice, the galvanometer mirror is rotated through about 10 degrees whilst monitoring the dc output of the photodiode to obtain the intensity-phase transfer function of the interferometer (ITF). The derivative of the ITF (a measure of the interferometric phase sensitivity) is then calculated and the mirror returned to that angle corresponding to the peak derivative - the point of maximum sensitivity. This procedure is repeated, prior to capturing the photoacoustic signal, for each point in the photodiode scan. Since the transfer function derivative provides a measure of the sensor sensitivity, it can be used to correct for any sensitivity variations due to changes in intensity across the illumination beam or imperfections in the sensing film. To implement this, the waveform captured at each point of the photodiode scan was divided by the peak value of the ITF derivative obtained at that point.

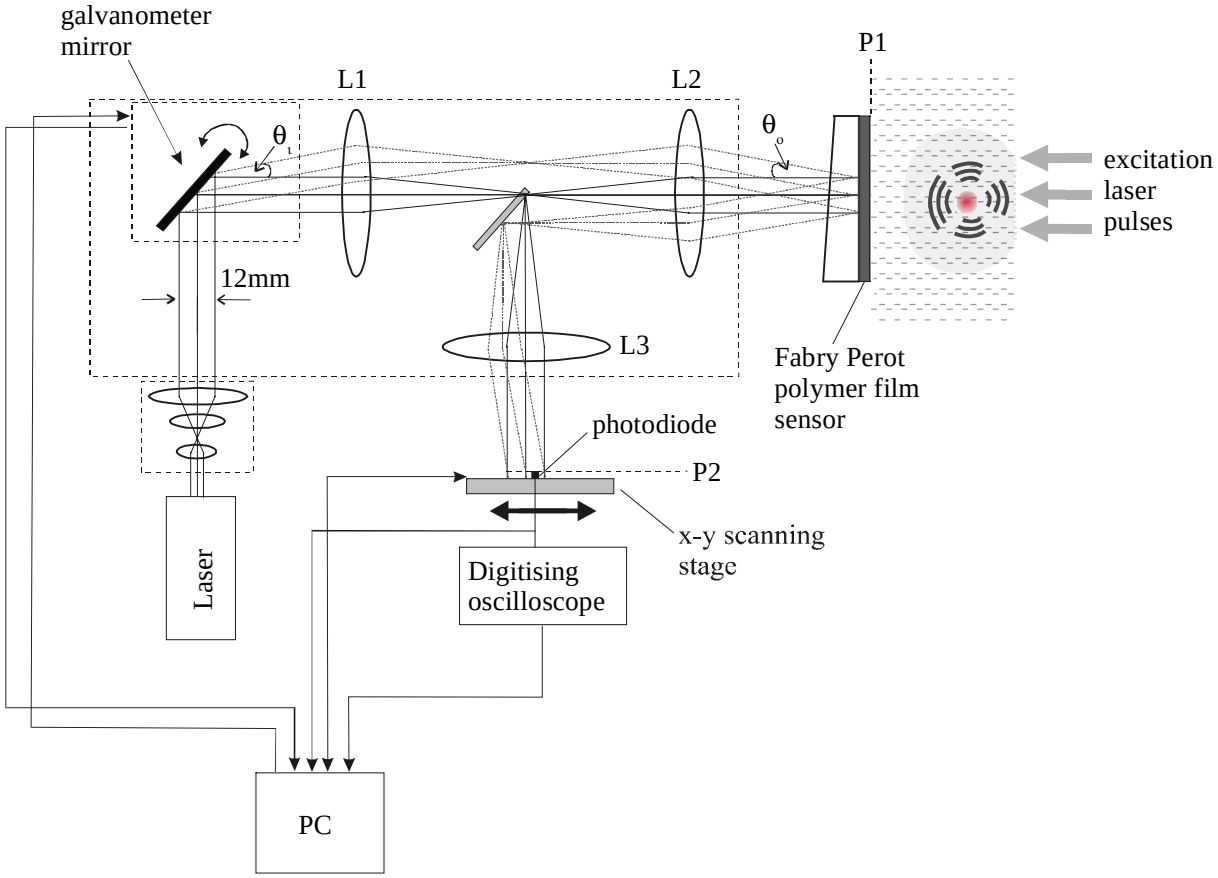

Figure 1 *Schematic of mechanically scanned transmission-mode photoacoustic imaging set-up. The galvanometer mirror, L1, L2 and L3 form the angle tuned phase bias control system for optimising sensitivity.*

The opacity of the sensor head to due to the aluminium coatings used to form the mirrors of the interferometer required the use of the transmission mode photoacoustic imaging configuration shown in figure 1. Although it provides a convenient and essentially equivalent means of initially evaluating the concept, the reflection mode of operation in which the photoacoustic signals are detected on the irradiated side of the target is generally required for biomedical applications. In future this will be achieved by using wavelength selective dielectric coatings that are transmissive to the pulsed excitation laser wavelength but reflective to the cw sensor interrogating wavelength to form the interferometer mirrors.

3. RESULTS

Experiments in phantoms comprising various absorbing structures immersed in a scattering liquid were performed using the arrangement shown in figure 1. In each case the background scattering liquid was a 10% aqueous solution of Intralipid-10% of approximately reduced scattering coefficient $\mu_s' = 1\text{mm}^{-1}$ and absorption coefficient $\mu_a = 0.03\text{mm}^{-1}$ at 1.06μm - the excitation wavelength used for these experiments.. These optical properties are approximately representative of tissues such as the breast[12] and skin[13] . The phantoms were irradiated with 30mJ optical pulses of 7ns duration emitted by a Q switched Nd:YAG laser. A negative lens was used to expand the laser output beam to a diameter in excess of 8mm to ensure that the incident surface fluence was always less than 0.1J/cm^2 - the maximum permitted exposure (MPE) level for nanosecond pulsed laser irradiation in the NIR incident on skin[14]. A linear grayscale mapping was used for all of the images shown in this paper.

3.1 Depth profiling of absorbing layers

To assess the maximum penetration depth at which a photoacoustic signal originating from a blood vessel might be detected,

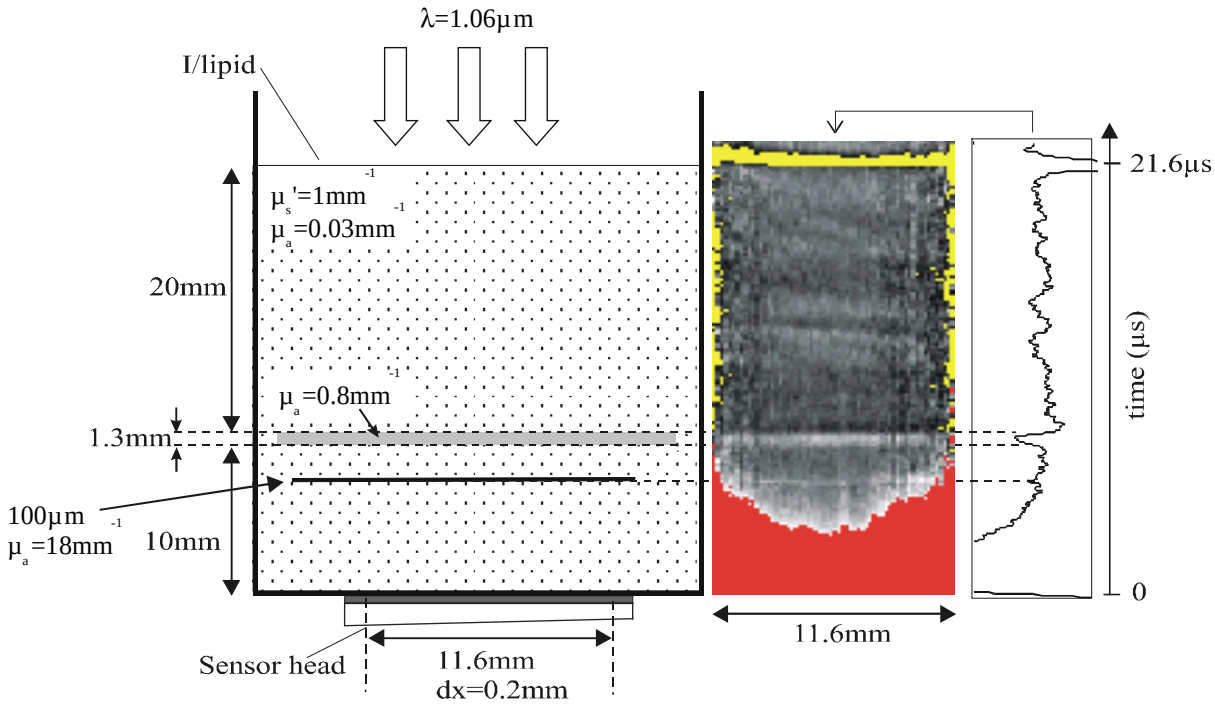

Figure 2 *Transmission-mode depth profiling of polymer absorbing layers in Intralipid phantom. The waveform on the far right shows a photoacoustic signal captured at the centre of the scan. The signal arriving at t=21.6µs (shown as a light thresholded band in the image) is generated at the surface of the Intralipid. The large low frequency component at t~0 (shown as the dark thresholded region in the image) is due to the heating of the sensing film by the excitation laser pulses. Scan step: 0.2mm, detector aperture: 0.8mm, incident laser fluence: 0.1J/cm^2, pulse duration=7ns*

2 plastic sheets, one of thickness 1.3mm and absorption coefficient μ_a=0.8mm^{-1} and the other 100µm thick and of μ_a=18mm^{-1} were submerged to a depth of 2cm in the Intralipid solution (figure 2) The absorption coefficient of the 1.3mm thick absorber was chosen to provide an absorption contrast comparable to that of fully oxygenated blood at 1.06µm[15].The purpose of the more strongly absorbing 100µm target was to provide a means of estimating axial spatial resolution rather than be representative of any particular tissue-optical properties. The excitation laser beam was incident on the surface of the Intralipid and the photacoustic signals were detected by the sensor head at the bottom of the water bath. The photodiode (aperture=0.8mm) was scanned along a line of length 11.6mm in 0.2mm steps across the sensor output beam. At each point of the scan, the detected time-dependent photoacoustic waveform was averaged over 200 shots and captured. To simulate the frequency dependent attenuating effects of soft tissues, an appropriate low pass filter (corresponding to a depth of 2cm) was applied to the detected signals. Each signal was then spatially resolved using the speed of sound, linearly mapped to a grayscale and vertically backprojected along the line-of-sight of the detector position at which it was captured to provide the image shown in figure 2. Figure 2 shows that signals from both plastic absorbers can be identified. The position and thickness and depth profile of 1.3mm absorber is in agreement with the known values. Although axial spatial resolution in this example is dominated by the low pass filtering applied to the signals, previous similar experiments[7] indicate the detector bandwidth is sufficient to resolve with sub-100µm resolution.

3.2 2D and 3D imaging of 62.5µm blood vessel phantoms

Various blood vessel phantoms using 62.5µm PMMA (polymethylmethacrylate) tubing containing an absorbing liquid or human blood were used in a set-up similar to that depicted in figure 2. Given the curvature of the wavefronts emitted by a source of such small dimensions, the line-of-sight imaging approach of section 3.1 is not appropriate if acceptable lateral resolution is to be achieved. Instead, a more generally applicable approach to image reconstruction was employed. In this, the assumption is made that the photoacoustic signal detected at a particular point in a 2D detector scan, at a specific time, emanates from points lying on a hemispherical surface, centred on the detector element, and of radius equal to the product of the source-detector transit time and speed of sound[16]. By radially backprojecting the spatially resolved time record of each element over a 2π solid angle, the original stress distribution and hence absorbed laser energy distribution can, in principle, be recovered to form a 3D image[17]. Unlike the line-of sight approach which requires a highly directional detector, it is necessary to spatially sample the incoming wavefront using a detector with an omnidirectional

response to minimise artefacts in the reconstructed image. This requires the detector element to be small compared to the acoustic wavelength – ideally a few tens of µm for short range applications such as imaging the skin where the frequency content of the photoacoustic signal can extend to several tens of MHz. Due to the limited sensor interrogating laser power available, the smallest aperture that could be placed in front of the photodiode to reduce the element size depended upon the detection sensitivity required. For the relatively large signals obtained when using india ink as the absorber (section 3.2.1), a 0.1mm aperture was used. To obtain adequate signal to noise ratio with the much more weakly absorbing blood (section 3.2.2), a 0.4mm aperture was necessary.

3.2.1 Preliminary experiments using india ink absorber

To initially evaluate the image reconstruction approach described above and obtain an indication of the spatial resolution that could be achieved with the smallest aperture of 0.1mm and an "array aperture" (the dimensions of the detector scan) of approximately 1cm, the arrangement in figure 3 was used. It comprises a length of 62.5µm PMMA tubing filled with india ink and positioned 1.7mm above the detection plane and 9mm beneath the surface of the Intralipid solution. An 8mm linescan in steps of 0.2mm was performed. Figure 3(a) shows a grayscale image of the detected acoustic signals in which the shape of the cylindrical wavefront emitted by the tube can just be discerned.

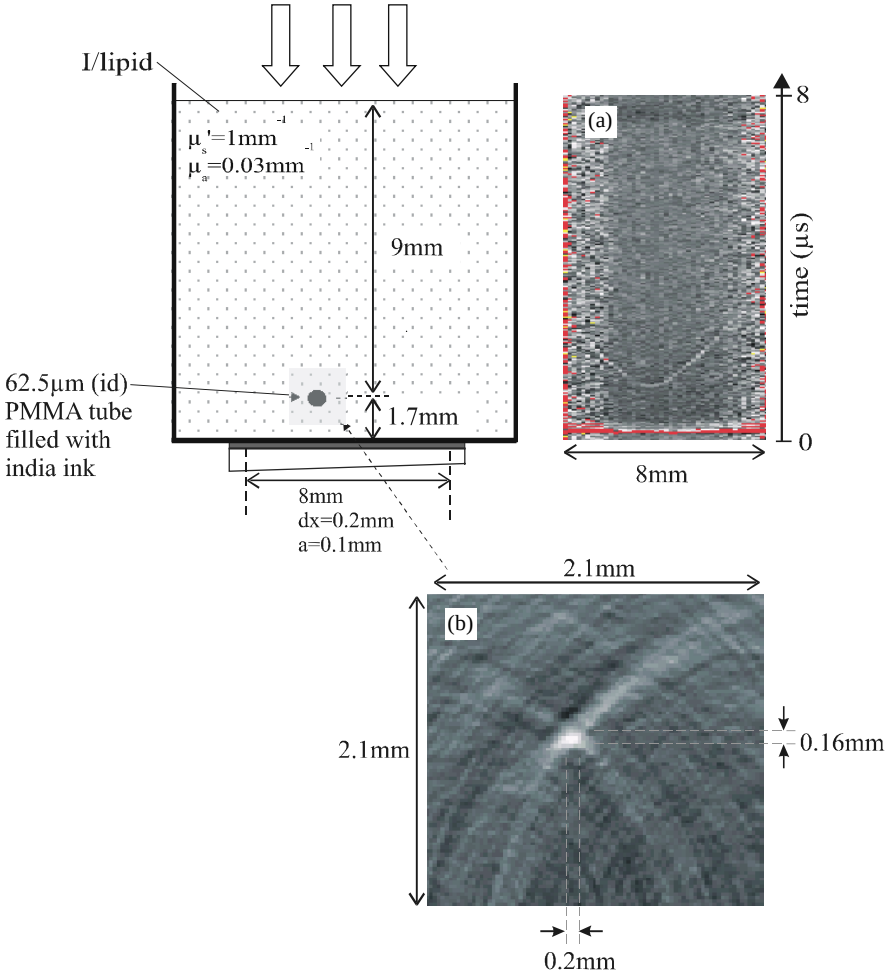

Figure 3 *2D imaging of india ink filled 62.5µm tube. (a) shows the detected photoacoustic signals and (b) shows the reconstructed image over a 2.1 x 2.1mm area centred on the tube – the shaded region in the schematic. Scan step: 0.2mm, detector aperture: 0.1mm, incident laser fluence: 0.1J/cm^2, pulse duration=7ns*

Figure 3(b) shows the image reconstructed from these signals by radially backprojecting them over 180 degrees into the plane of the linescan Strictly, the detector should have been scanned over 2D rather than 1D and the backprojection carried out over a 2π solid angle to perform a 3D reconstruction. Otherwise it is not generally possible to localise in the vertical direction. The photoacoustic signals could have originated from any point on an arc centred on the detection point

and in a plane perpendicular to that of the linescan. However in this case, the tube was deliberately aligned so that it was parallel to the detection plane, enabling the assumption to be made that no out of plane signals were detected. In doing so, the reconstruction problem is reduced to one of 2 dimensions enabling a linescan to be used for rapid data acquisition for evaluation purposes. The reconstructed image in figure 3(b) clearly shows the tube with good contrast. Around it, backprojection arcs, due to the limited aperture over which the wavefront is sampled, can just be observed. Spatial resolution, for a given acoustic frequency content, is defined by the length of the scan, the detector element size and bandwidth and distance of the source from the detection plane. As figure 3(b) shows, the lateral resolution is 0.2mm and the axial resolution 0.16mm.

3.2.2 Experiments using human blood

An arrangement in which a single length of the 62.5µm PMMA tubing was threaded through a rectangular frame to produce three diagonally located targets as shown in figure 4 was used. Blood, extracted from the fingertip of the author was then introduced into the tube and the whole arrangement immersed in the Intralipid solution..

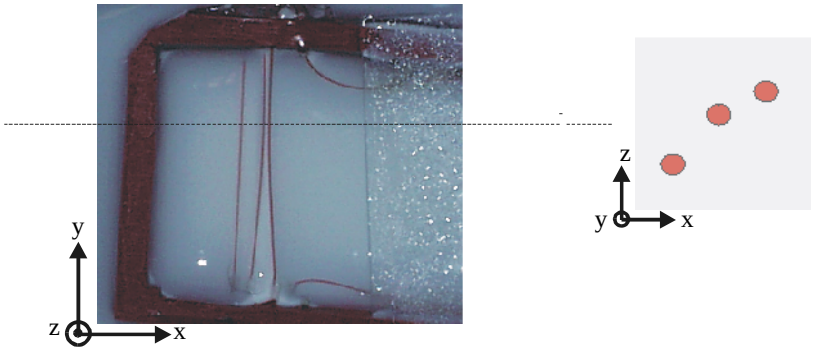

Figure 4 *Photograph of top view of 3 line 62.5µm blood vessel phantom prior to immersion in Intralipid and (right) schematic of vertical section through dashed line.*

Due to the much lower absorption coefficient of blood compared to india ink, greater detection sensitivity was required. Therefore the photodiode aperture was increased to 0.4mm. The detected photoacoustic signals were bandpass filtered (0.6 – 12MHz) to (a) reduce the low frequency contribution due to the heating of the sensor film by the absorption of the laser pulse and (b) improve signal-noise ratio by limiting the overall measurement bandwidth to the acoustic frequency response of the sensor. 2D and 3D images were obtained by performing 1D and 2D detector scans respectively as described below.

3.2.2.1 2D image Figure 5 shows the position of the tubes within the Intralipid. A 2D image was obtained by linescanning the photodiode over 8mm in steps of 0.1mm and reconstructing as described in section 3.2.1. Figure 5(a) shows the detected photoacoustic signals. The cylindrical wavefronts emitted by the three tubes at different depths are clearly visible. The horizontal line (H) and the tilted line (T) are reflections, from within the sensor head, of the photoacoustic signal generated by the strong absorption of the laser pulse in the external aluminium coating of the sensor. From these the wedge shaped structure of the sensor is discernible. W represents the signal generated at the surface of the Intralipid. The thresholded region close to t=0 represents the remainder of the thermal signal after filtering.

Figure 5(b) shows the image reconstructed over a 3.75 x 3.75mm area. The three tubes are clearly visible. The horizontal line just below centre is the reconstruction of the artefactual signal H. The lateral resolution is approximately 0.33mm - lower than that of figure 3 due to the increased detector size (0.4mm) and the greater distance from the detection plane. The depth resolution for this source-detector distance is largely dominated by the detector bandwidth and remains at approximately 0.15mm.

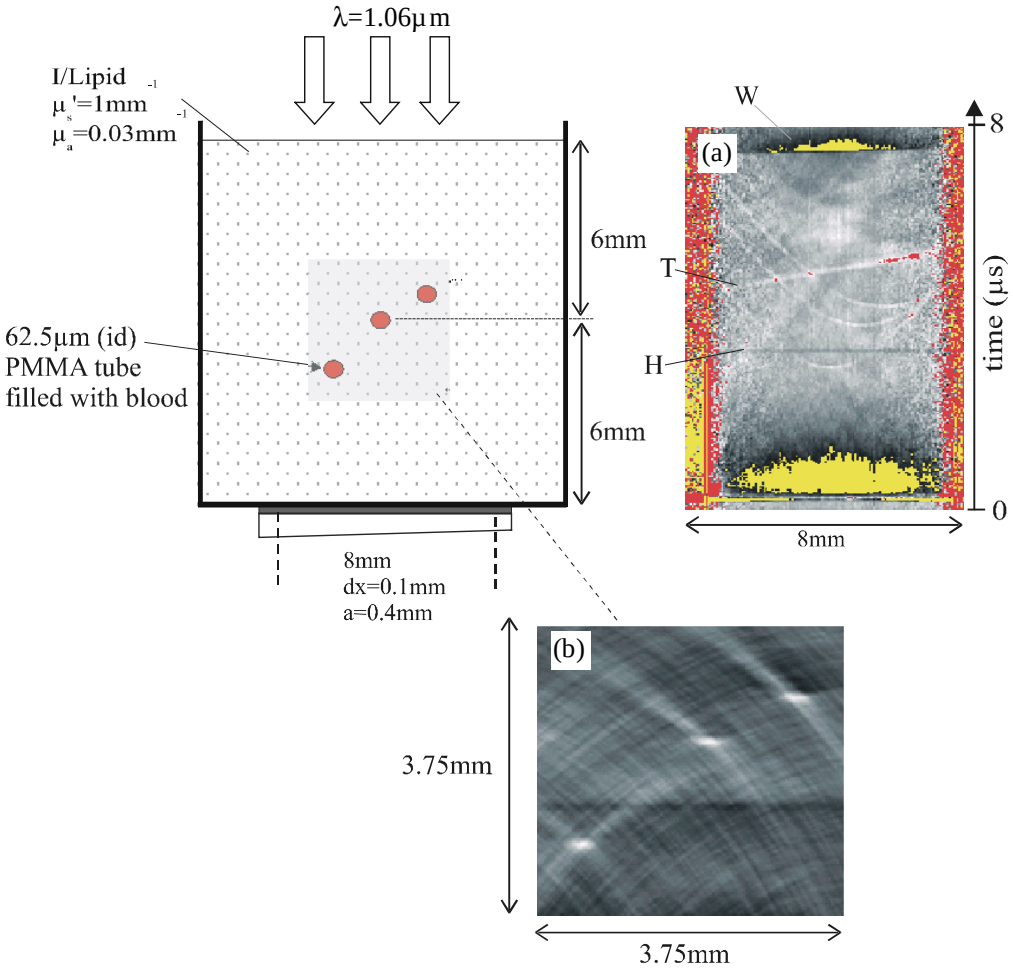

Figure 5 *2D imaging of 3 line 62.5µm blood vessel phantom. (a) shows the detected photoacoustic signals. The cylindrical wavefronts originating from the three tubes are clearly visible. W is the signal generated in the surface of the intralipid, T and H are reflections within the sensor head of the signal generated in the external aluminium coating of the polymer sensing film. (b) shows the reconstructed image over a 3.75 x 3.75mm area.. Scan step: 0.1mm, detector aperture: 0.4mm, incident laser fluence: 0.1J/cm^2, pulse duration=7ns*

3.2.2.2 3D Image The above experiment was repeated. However, instead of the linescan, the detector was scanned over a rectangular surface of 6 x 6mm in steps of 0.2mm using a detector aperture of 0.4mm. A 3D image was reconstructed over a 6 x 5 x 3.5mm volume by radially backprojecting the 2D distribution of detected photoacoustic signals over a 2π solid angle as described in section 3.2. The geometry of the detection scan and the reconstruction volume is illustrated in figure 6. Some additional high pass filtering was performed on the reconstructed image to remove the remaining early low frequency thermal signal component which otherwise produces a large background level that reduces contrast. Figure 7 shows vertical (*y-z*) sections and figure 8 horizontal sections (*x-y*) through the reconstructed volume at positions corresponding to the centres of each tube. The three vessels can clearly be seen. The lateral resolution at 0.4mm is lower than that observed in figure 5. This is largely due to the reduced dimensions of the scan (ie array “aperture”) and number of steps. The axial resolution remains at 0.15mm.

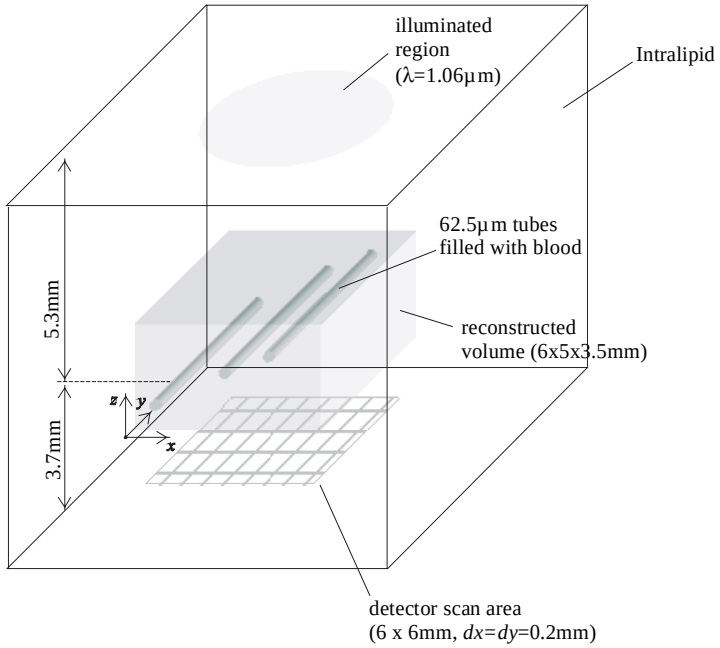

Figure 6 *Geometry for 3D image reconstruction of 3 line 62.5μm blood vessel phantom immersed in Intralipid solution (μ_s =1mm^{-1}, μ_a=0.03mm^{-1}) – the lowest tube is 5.3mm beneath the surface of the Intralipid. The photodiode was scanned over a 6 x 6mm surface in steps of 0.2mm using a 0.4mm aperture and the reconstruction performed over a 6 x 5 x 3.5mm volume.*

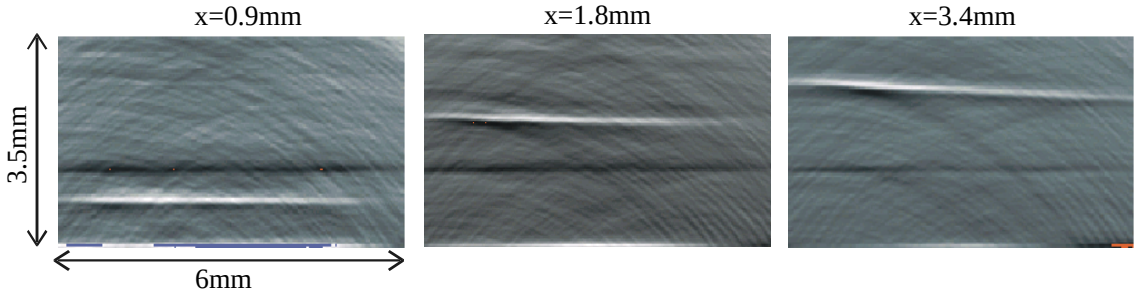

Figure 7 *Vertical (y-z) sections through the reconstructed volume shown in figure 6 moving from left to right in the positive x-direction showing the relative vertical positions of the three blood filled tubes. The dark horizontal line at the same position in each image is the reconstruction of the sensor reflection artefact H shown in figure 5(a)*

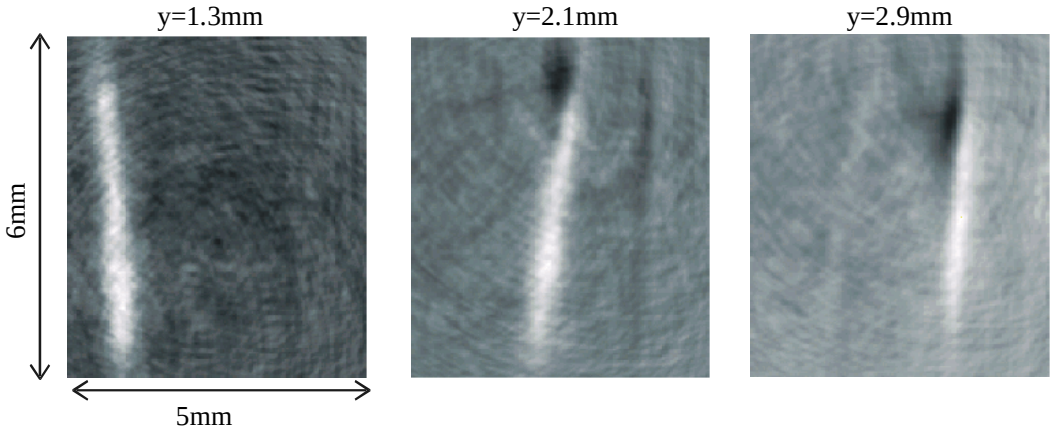

Figure 8 *Horizontal (y-x) sections with increasing height through reconstructed volume showing the relative lateral positions of the 3 tubes.*

4. CONCLUSIONS

The feasibility of using the Fabry Perot polymer film sensing concept for photoacoustic imaging of blood vessels to depths approaching 1cm has been demonstrated. The lateral resolution of a few hundred microns is currently limited by the detector aperture used. By using a higher power sensor interrogating laser to maintain detection sensitivity, it should be possible to reduce the aperture to improve this. There is also further scope to improve depth resolution (currently 150µm) by reducing the sensor film thickness to increase bandwidth. Future work is to concentrate on the development of the reflection mode sensor head (section 2) required for practical biomedical application and the use of a multielement array of photodiodes or CCD array[10,17] in place of the current mechanically scanned photodiode to reduce image acquisition time.

ACKNOWLEDGEMENTS

P. Beard is supported by an EPSRC Advanced Fellowship.

REFERENCES

[1] Kruger RA, Miller KD, Reynolds HE, Kiser Jr WL, Reinecke DR, Kruger GA. Contrast enhancement of breast cancer in vivo using thermoacoustic CT at 434 MHz. Radiology; 216: 279-283, 2000

[2] Andreev VG, Karabutov AA, Solomatin SV, Savateeva EV, Aleynikov V, Zhulina YV, Fleming RD, Oraevsky AA, Optoacoustic tomography of breast cancer with arc-array-transducer, *Proc* SPIE Vol 3916, pp36-47, 2000

[3] Hoelen CG, de Mul FFM, Pongers R, Dekker A, , Three-dimensional photoacoustic imaging of blood vessels in tissue, Optics Letters, Vol 23, No 8, pp648-650, 1998

[4] Paltauf G., Koestli K, Frauchiger D, Frenz M., Spectral optoacoustic imaging using a scanning transducer, Proc. SPIE Vol. 4434, p. 81-88, 2001

[5] Beard PC and Mills TN, A 2D optical ultrasound array using a polymer film sensing interferometer, 2000 IEEE Ultrasonics Symposium, pp1183-1186, 2000

[6] Beard PC and Mills TN, An optical detection system for biomedical photoacoustic imaging, Proc. SPIE 3916, pp100-109, 2000

[7] Beard PC and Mills TN, 2D line scan photoacoustic imaging of absorbers in a scattering tissue phantom, Proc SPIE 4256, pp34-42, 2001

[8] Beard PC, Perennes F, Mills TN, Transduction mechanisms of the Fabry Perot polymer film sensing concept for wideband ultrasound detection., *IEEE Transactions on Ultrasonics, Ferroelectrics and Frequency control*, Vol 46, No 6, pp1575-1582, 1999

[9] Beard PC, Hurrell A, Mills TN, Characterisation of a polymer film optical fibre hydrophone for the measurement of ultrasound fields for use in the range 1-20MHz: a comparison with PVDF needle and membrane hydrophones, *IEEE Transactions on Ultrasonics, Ferroelectrics and Frequency control*, Vol 47, No1, p256-264, 2000

[10] Paltauf G and Schmidt-Kloiber H, Optical method for two dimensional ultrasonic detection, Applied Physics Letters, Vol 75, No 8, pp1048-1050, 1999

[11] Wilkens V. and Koch Ch., Optical multilayer detection array for fast ultrasonic field mapping, Optics Letters, Vol 24, No 15, pp1026-1028, 1999

[12] Troy TA, Page DL, Sevic-Mucraca EM, Optical properties of normal and diseased breast tissues: prognosis for optical mammography, J Biomed Optics, 1(3), pp342-355, 1996

[13] Simpson, C.R., Kohl, M., Essenpreis, M., Cope, M., "Near-infrared optical properties of ex vivo human skin and subcutaneous tissues measured using the Monte Carlo inversion technique," Phys. Med. Biol. 43, 2465-2478 (1998).

[14] British Standard, BS EN60825-1, 1994

[15] Roggan A, Friebel M, Dorschel K, Hahn A, Muller G, Optical properties of circulating human blood in the wavelength range 400-2500nm, Journal of Biomedical Optics, 4(1), pp36-46, 1999

[16] Landau LD and Lifshitz EM, Fluid Mechanics, 2nd edition, Butterworth Heinemann

[17] Koestli K, Frenz M, Weber HP, Paltauf G, Schmidt-Kloiber H, Optoacoustic tomography: time-gated measurement of pressure distributions and image reconstruction , Applied Optics, Vol. 40, No 22, pp3800-3809, 2001